

Title no. 97-S39

## Models for Laterally Loaded Slab-Column Frames

by Shyh-Jiann Hwang and Jack P. Moehle

Effective beam width and equivalent frame models are commonly used in design to model the lateral load response of slab-column frames. An analytical evaluation of these two models is made, considering effects of connection and panel geometry, as well as effects of cracking on frame stiffness. Models suitable for design office implementation are recommended. Results of the recommended models are compared with experimental data obtained from tests of a 0.4-scale, multipanel, slab-column frame.

**Keywords:** buildings; deflection; design; frames; loads; models; moments; reinforced concrete; slabs; stiffness; tests.

### INTRODUCTION

A range of analytical procedures exists for modeling slab-column frames subjected to lateral loads.<sup>1</sup> Such models are important to designers of multistory buildings in that they enable lateral drifts to be calculated. In high-rise construction where the slab-column frame is braced by structural walls, analytical models gain additional importance in that they determine design interactions between the frame and wall, and hence, the required strengths of the two subsystems. As described by Vanderbilt and Corley,<sup>1</sup> available analytical models do not produce the same result; rather, the stiffness obtained from one type of analytical model can vary widely from that of another, and both may be far from actual behavior.

The present study is concerned with two analytical models that are commonly used in design-office practice. These are the effective beam width model, in which the slab action is represented by a flexural slab-beam framing directly between columns (Fig. 1), and the equivalent frame model, in which the slab action is represented by a combination of flexural and torsional beams (Fig. 2). Characteristics of both models are discussed, and recommendations on proper application are made. The recommendations are based on a detailed experimental and analytical evaluation presented elsewhere.<sup>2,3</sup> The recommended analytical models are tested by comparison with results obtained on lateral load experiments of a multipanel test slab.<sup>2,3</sup>

### FRAME MODELS FOR MULTISTORY BUILDINGS

An analytical model for interpretation of structural response should be constructed in sufficient detail that actions of interest are reasonably reproduced; analytical detail beyond this level may be counterproductive, as it can decrease efficiency in model preparation, numerical computation, and, most importantly, interpretation. With these guidelines in mind, a model of a three-dimensional building is usually assembled using line elements for columns and floor members. Vanderbilt and Corley<sup>1</sup> discuss techniques for representing a symmetric building using planar frames and planar analysis. Analyses of complete three-dimensional space frames consisting of line elements for beams and floor members are readily accomplished using available computer codes.

A simple three-dimensional building and a space frame analytical model of the building are depicted in Fig. 3. It is common practice to represent the relatively stiff volume of concrete common to the beams and columns (the joint) by rigid zones. The

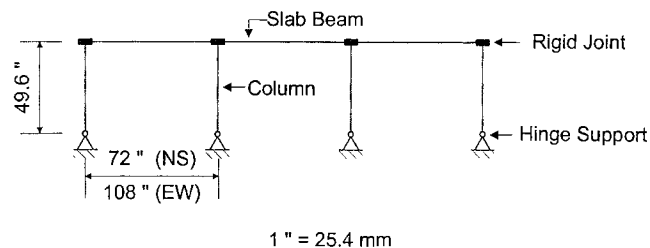


Fig. 1—Effective beam width model.

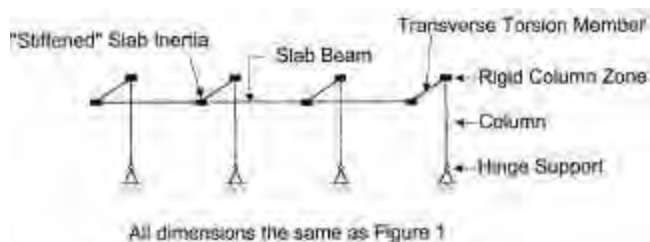


Fig. 2—Equivalent frame model.

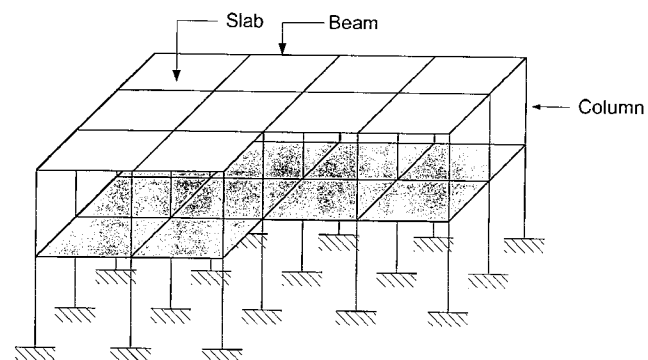


Fig. 3—Frame model of three-dimensional building.

line elements representing the columns may be assigned the flexural, shear, and axial properties of the columns. Though consideration of possible stiffness reduction due to cracking is appropriate, the column is often assigned properties based on gross concrete sections. In any building construction involving monolithic floor slabs, determination of the mechanical properties of the floor members is less direct. It is the determination of these properties in slab-column construction that is the main object of this paper.

ACI Structural Journal, V. 97, No. 2, March-April 2000.

MS No. 99-155 received May 4, 1999, and reviewed under Institute publication policies. Copyright © 2000, American Concrete Institute. All rights reserved, including the making of copies unless permission is obtained from the copyright proprietors. Pertinent discussion will be published in the January-February 2001 ACI Structural Journal if received by September 1, 2000.

Shyh-Jiann Hwang is a professor in the Department of Construction Engineering, National Taiwan University of Science and Technology, Taipei, Taiwan.

Jack P. Moehle is a professor of civil engineering and Director of the Pacific Earthquake Engineering Research Center, University of California, Berkeley, Calif.

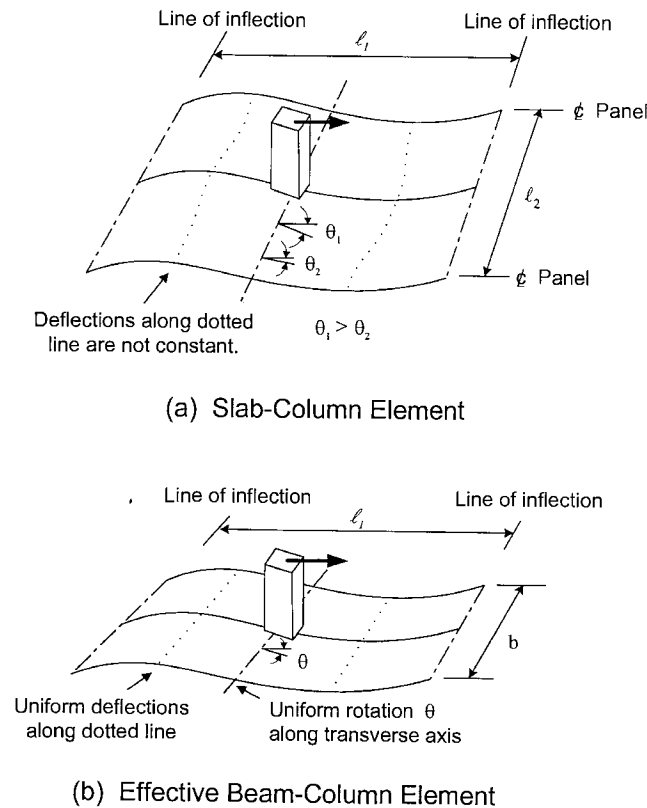


Fig. 4—Concept of effective beam width model.

## EFFECTIVE BEAM WIDTH MODEL

### Description of model

In slab-column construction, the slab is not fully effective across its full width as a flexural element framing into the column. The behavior of a typical connection is illustrated in Fig. 4(a). As shown in that figure, when the connection is subjected to rotation, the slab near the column rotates with the column. More distant portions of the slab (along the transverse centerline of the connection) do not experience the same rotation. Because of computational difficulties in precisely modeling the three-dimensional behavior of the slab in a complete building analysis, it is commonplace in design to model the slab in a simplified manner.

In one simple model, the effective beam width model, the actual slab is replaced with a slab-beam element that rotates uniformly across its transverse width (Fig. 4(b)). The slab-beam element has a thickness equal to that of the slab, and an effective beam width equal to some fraction of the actual slab transverse width. Numerous analytical and experimental techniques for obtaining the effective beam width have been proposed, producing almost an equally large number of results.<sup>4-12</sup> A summary of several solutions is presented by Vanderbilt and Corley.<sup>1,13</sup> A common assumption in calculating effective beam widths is that lines of inflection are located along slab midspans perpendicular to the bending direction, as shown in Fig. 4. The solutions also commonly assume elastic plate behavior. The solutions vary in their treatment of the joint region; some consider the slab to be flexurally rigid within the plan of the column, while others assign a joint flexibility equal to that of the surrounding slab. Solutions obtained assuming the joint to be either rigid or flexible are plotted

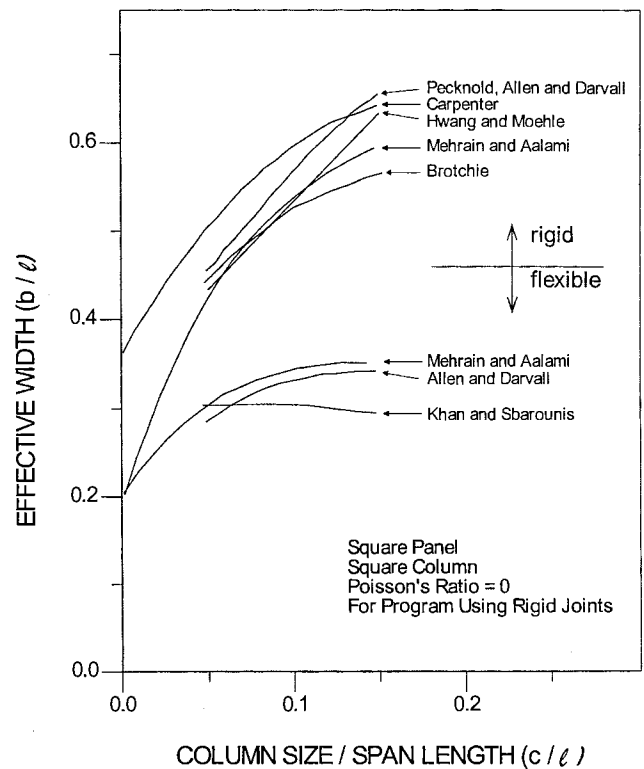


Fig. 5—Summary of effective beam width for lateral loading.

in Fig. 5. Test results have demonstrated that the rigid joint assumption better represents an elastic slab-column joint.<sup>5,11</sup>

Even if the rigid joint assumption is selected as the preferred solution for an elastic slab, it is apparent (Fig. 5) that a range of solutions has been obtained by various researchers. This range arises from differences in modeling techniques relative to the slab, the rigid joint, and the boundary around the rigid joint.<sup>2,14</sup>

In the interest of establishing effective widths that accurately represent the elastic behavior of a slab-column connection having a rigid joint, an independent solution has been pursued.<sup>2</sup> The solution employs the infinite plate theory of Westergaard<sup>15</sup> to model an infinite plate having columns with circular cross sections on a regular layout. Rigid joint behavior is strictly enforced. Results of the solution were checked using the finite element method. (Details of both solutions are in the Appendix.\*)

Two important conclusions result from the solutions presented in the Appendix. First, the new solutions indicate effective widths that are somewhat less than values presented elsewhere.<sup>5,10</sup> Darvall and Allen obtained a similar finding in an independent study.<sup>14</sup> The second conclusion is that the finite element technique employed in the analysis produced solutions nearly equal to those of the theoretical solution. This latter conclusion is important because the finite element method can be used to determine effective widths for connection and panel geometries for which the theoretical solution does not apply. Results of the finite element analyses of typical slab-column floor connections are described in the following section.

### Elastic effective widths

Banchik presents effective width solutions developed using the finite element technique as described previously.<sup>16</sup> The solutions apply to interior, edge, and corner connections, for columns

\*The Appendix is available in xerographic or similar form from ACI headquarters, where it will be kept permanently on file, at a charge equal to the cost of reproduction plus handling at time of request.

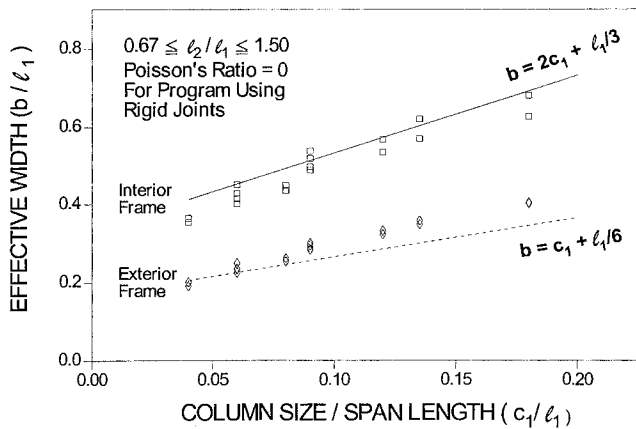


Fig. 6—Effective beam width by Banchik using finite element

with square cross sections, and for combinations of  $c_1/l_1$  and  $l_2/l_1$ , defined as follows

$$c_1/l_1 = 0.06, 0.09, 0.12$$

$$l_2/l_1 = 0.67, 1.00, 1.50$$

Results of Banchik's study are presented in the Appendix.\* For the exterior connections, two series of analyses were performed. In one series, the plate edge was flush with the outside face of the column. Results of this series and of interior connection analyses will be addressed in next paragraph. The other series of exterior connections considered flat plates with overhangs;<sup>16</sup> these are not considered further herein.

Banchik presented his results using  $c_1/l_2$  as the main geometric variables. His results are plotted in terms of  $c_1/l_1$  in Fig. 6. The results apparently fall into two distinct groups: one for the interior frame and one for the exterior frame. The variation of the effective beam width  $b$  for an interior frame, which includes interior connections and edge connections with bending perpendicular to the edge, can be represented as

$$b = 2c_1 + \frac{l_1}{3} \quad (1)$$

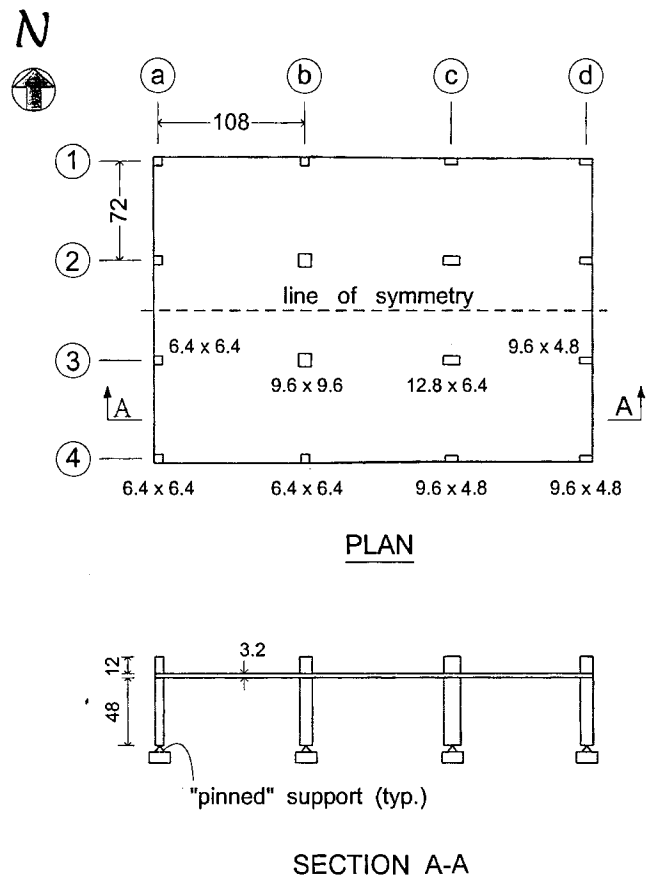
As demonstrated in the Appendix,\* Eq. (1) can be justified using Westergaard's infinite plate theory.<sup>15</sup> The effective beam widths for an exterior frame, which includes corner connections and edge connections with bending parallel to the edge, can be approximated as

$$b = c_1 + \frac{l_1}{6} \quad (2)$$

According to these expressions, the theoretical effective beam width of a connection in the exterior frame (Eq. (2)) is half the value for the same connection in the interior frame (Eq. (1)).

Both Eq. (1) and (2) are derived with zero Poisson's ratio ( $\nu = 0$ ). A multiplier of  $1/(1 - \nu^2)$  can be applied to account for effects of Poisson's ratio,<sup>10</sup> though the effect is small and can be ignored. Further, the values from Eq. (1) and (2) are applicable to frame models in which the joint is modeled as being rigid, as in Fig. 1. If rigid joints are not included in the frame model, the

\*The Appendix is available in xerographic or similar form from ACI headquarters, where it will be kept permanently on file, at a charge equal to the cost of reproduction plus handling at time of request.



(All units are in inches, 1 in. = 25.4 mm)

Fig. 7—Layout of UCB test slab.

widths given by Eq. (1) and (2) should be modified by the factor  $1/(1 - \nu^2)$ .

In Eq. (1) and (2), only the geometric parameters  $c_1$  and  $l_1$  are involved. The importance of the ratio  $c_1/l_1$  has been identified by Mehrain and Aalami,<sup>9</sup> Pecknold,<sup>10</sup> and Allen and Darvall.<sup>5</sup> Pecknold<sup>10</sup> examined the effect of column rectangularity by varying the ratio  $c_2/c_1$  from 1/2 to 2, and found it negligible within this range. Allen and Darvall<sup>5</sup> studied the influence of  $c_2$  for a range of values of  $c_2/l_1$  from 0.03 to 0.12 and found its effect to be negligible. Pecknold indicated in his discussion with Glover<sup>10</sup> that the aspect ratio ( $l_2/l_1$ ) is of little importance relative to the connection stiffness if  $l_2/l_1$  is greater than 3/4. A similar finding has been reported elsewhere.<sup>9,17</sup> These observations are consistent with Eq. (1) and (2).

The validity of Eq. (1) and (2) can be further checked by comparison with stiffnesses calculated for multipanel floor slabs using the finite element method. One of the floor slabs analyzed is a slab that was tested experimentally at the University of California, Berkeley<sup>2,3</sup> (Fig. 7). The structure has square and rectangular cross section columns, and slab panels with an aspect ratio of 1.5 to 1. The model is first analyzed for translation (and, effectively, load) in the NS direction ( $l_2/l_1 = 1.5$ ). Three additional slab models are analyzed; these are identical to the model shown in Fig. 7 in every respect except the transverse span is varied resulting in slab panel aspect ratios of  $l_2/l_1 = 0.75, 1.0$ , and 2.0.

In the finite-element model, the slab-column frames (Fig. 8) were modeled by 989 QUAD elements<sup>18</sup> using the SAP80 computer package.<sup>19</sup> Shear and axial deformations were neglected. Poisson's ratio  $\nu$  was taken equal to 0.15. Plates in joint regions were made effectively rigid, having a stiffness six orders of magnitude greater than plates outside the joints. The slab-column frames were also modeled using the effective beam width model

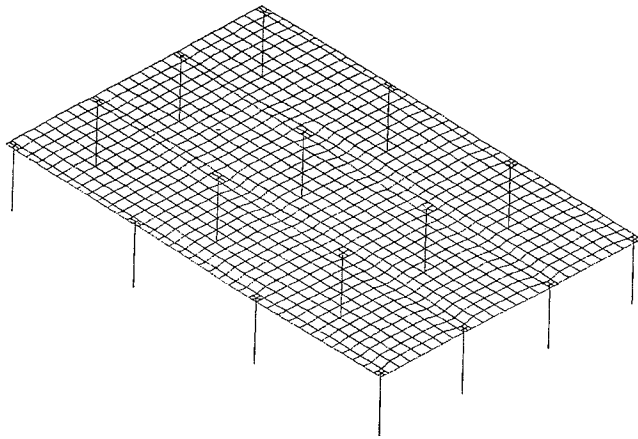


Fig. 8—Finite element model of UCB test slab.

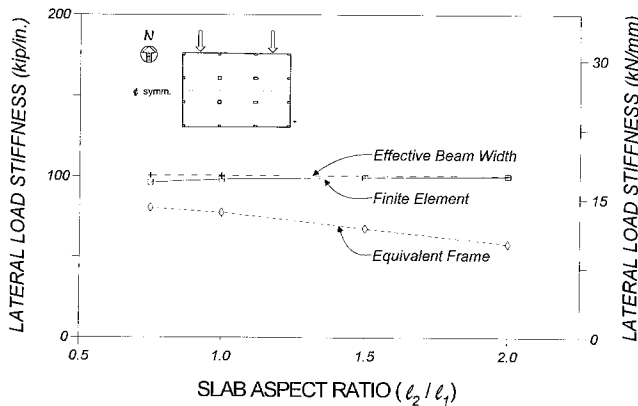


Fig. 9—Evaluation of lateral load models (NS-Dir.).

(Fig. 1). The effective beam widths are those recommended by Eq. (1) and (2), modified as described previously to account for Poisson's ratio. For both analytical models, columns are modeled by beam-column elements having cracked section properties (Table 1). Rigid slab-column joints are specified.

Figure 9 summarizes the computed lateral-load stiffnesses of the four slab-column frames that differ only in transverse span length, as described previously. The finite element results (continuous curve in Fig. 9) indicate that the transverse span length ( $\ell_2$ ) has little effect on the lateral-load stiffness of an elastic plate. With increasing  $\ell_2$ , lateral-load stiffness increases only slightly within the range considered. This observation is consistent with the slab deformation pattern sketched in Fig. 4. Results computed using the effective beam width model (Fig. 9) follow closely the finite element results, indicating that the proposed expressions for effective width (Eq. (1) and (2)) adequately represent the elastic lateral stiffness of the flat-plate structure.

An assumption common in the derivation of effective beam widths is that lines of inflection occur along panel midspans under lateral loads (Fig. 4). This assumption is nearly correct for NS loads applied to the slab-column frame of Fig. 7 because connections along a given frame line have nearly equal stiffness. If loads are applied in the EW direction of that frame, the inflection lines will not be located near midpanels because the different column geometries along frame lines result in unequal connection stiffnesses. Effective widths derived for the inflection line at the midspan add a constraint to the solution, and thus will artificially stiffen the frame.

To illustrate this phenomenon, the slab described in Fig. 7 was analyzed for loads in the EW direction ( $\ell_2/\ell_1 = 0.67$ ). Three additional frames identical to the previously mentioned slab, but with  $\ell_2/\ell_1 = 1.0, 1.5,$  and  $2.0,$  were also analyzed. In the analyses, the effective width for each connection was calculated in-

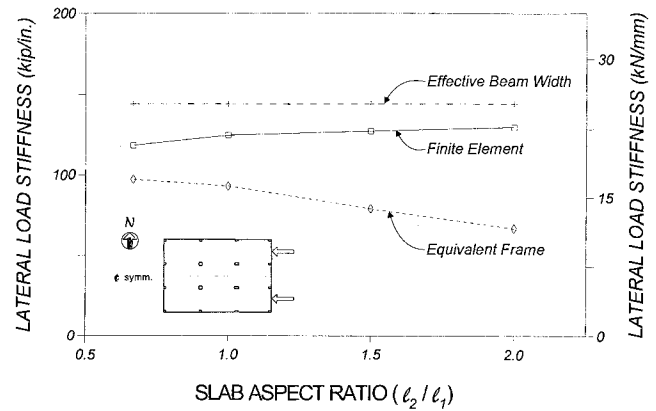


Fig. 10—Evaluation of lateral load models (EW-Dir.).

Table 1—Cracked moment of inertia of columns

Column size, in.	6.4 x 6.4	4.8 x 9.6	9.6 x 9.6	6.4 x 12.8
NS dir., in. <sup>4</sup>	120	75	420	240
EW dir., in. <sup>4</sup>	120	320	420	1000

Note: 1 in. = 25.4 mm

dependently, and then the widths for the two columns of a given span were averaged to obtain the effective width for the span. Results of the analyses (Fig. 10) illustrate that the effective beam width solution is indeed artificially stiff. A similar stiffening effect is likely to occur whenever the effective beam width solution is applied to irregular framing. In this context, irregular framing includes variation in span and variation in column cross section along the frame line.

Based on findings of the preceding analysis, Eq. (1) and (2) are recommended to represent the elastic effective beam widths of flat-plate connections having column aspect ratio  $c_2/c_1$  between  $1/2$  to  $2,$ <sup>10</sup> and slab aspect ratio  $\ell_2/\ell_1$  greater than  $2/3$ <sup>16</sup> (Fig. 6). The previously-mentioned range of geometries is not exhaustive, but includes most of the slab configurations in practice. The recommended solution will produce an accurate estimate of the elastic stiffness for regular frames. The solution will be artificially stiff for irregular frames.

### Effects of cracking on connection stiffness

Experimental data obtained from lateral load tests on isolated slab-column connections and complete slab-column frames have consistently indicated stiffnesses well below the theoretical elastic stiffnesses.<sup>1-3,20-23</sup> The stiffness reduction is illustrated for one case in Fig. 11. The measured stiffness corresponds to readings from a vertical and lateral load test of a flat-plate frame, as reported by Moehle and Diebold.<sup>20</sup> The stiffness calculated using the effective beam width solution is shown by the continuous line in that figure. For the present example, the measured stiffness at drift of  $0.0025H,$  where  $H$  is the column height, is approximately half the calculated stiffness. This result is in the range typically observed.

The stiffness reduction illustrated in Fig. 11 has generally been attributed to cracking (visible or otherwise) of slab concrete. The cracking may arise from restrained volume changes and externally applied loads. That the reductions in stiffness are as large as they are in laboratory tests where construction load and volume change effects are minimized is particularly noteworthy; larger effects may be realized in field construction.

In their discussion of frame models, Vanderbilt and Corley<sup>1</sup> recognize the need to consider stiffness reductions due to slab cracking. Lacking laboratory data on large-scale structural models, they recommended use of a lower bound estimate of slab stiffness equal to  $1/3$  of the gross-section value. The stiffness res-

duction was specified to be applied to the slab-beam of the ACI equivalent frame model.

The reduction factor of 1/3 recommended by Vanderbilt and Corley is reasonable given the perspective that: a) slab-column connection stiffness is governed by slab flexural behavior; and b) the reduction in flexural stiffness due to externally applied loads seldom exceeds 1/3. Although it has never been clear that the moment-rotation behavior of a slab-column connection is governed by flexural action, or that the flexural stiffness of a cracked, lightly-reinforced slab is bounded on the lower end by 1/3 of the gross-section stiffness, the solution proposed by Vanderbilt and Corley has produced conservative and reasonable results.<sup>1,20,23</sup> As an example, the reduction factor of 1/3 is applied to the slab-beam of the effective beam width model for the slab reported by Moehle and Diebold,<sup>20</sup> and the resulting stiffness, plotted for comparison in Fig. 11.

In one study,<sup>2</sup> analytical and experimental data were used to evaluate more critically the lower bound solution of Vanderbilt and Corley. In the evaluation, the extent of flexural cracking adjacent to a slab-column connection under the action of gravity and lateral loads was estimated analytically. The effects of this load-induced cracking on connection stiffness were modeled using a finite element representation of the connection in which cracked regions of the slab (plate bending elements) were assigned a stiffness reduction equal to the ratio between the fully-cracked and gross-section flexural stiffnesses. The model was able to reproduce, with reasonable accuracy, the measured effects of increased loads on stiffness reduction for a variety of laboratory experiments. Details of the analytical model and correlations are presented elsewhere.<sup>2</sup>

Using the cracking model described in,<sup>2</sup> a parameter study was conducted in which an extensive series of slab-column connections was designed according to ACI 318-83,<sup>24</sup> and the maximum stiffness reduction due to cracking expected under service loads was calculated. It was found that the maximum stiffness reduction can be expressed as a function of the service live load, slab geometry, and material properties. Specifically, for a slab having  $f_c = 4000$  psi,  $f_y = 60$  ksi, the slab stiffness reduction factor is given by

$$\beta = 5 \frac{c}{\ell} - 0.1 \left( \frac{LL}{40} - 1 \right) \geq \frac{1}{3} \quad (3)$$

in which  $LL$  is the service live load in unit of  $\text{lb/ft}^2$  ( $40 \text{ lb/ft}^2 = 1915 \text{ Pa}$ ), and  $\beta$  is the ratio of the cracked to gross-section stiffnesses of the slab-beam in the effective beam width model. Further approximation aimed toward simplicity and conservatism results in the expression

$$\beta = 4 \frac{c}{\ell} \geq \frac{1}{3} \quad (4)$$

The lower bound value given by Eq. (3) and (4) (that is,  $\beta = 1/3$ ) matches that recommended by Vanderbilt and Corley.<sup>1</sup>

## EQUIVALENT FRAME MODEL

### ACI Code model

ACI 318-95<sup>25</sup> describes the equivalent frame model for gravity load analysis of two-way slab systems. As presented in the Code, the equivalent frame is an effectively planar frame, with properties defined to represent the relative framing stiffnesses under vertical loads. The equivalent frame model for a typical frame line of the slab shown in Fig. 7 is depicted in Fig. 2. As shown, the equivalent frame contains columns and slab-beams (directly representing the flexural stiffnesses of the columns and the slab). To simulate the framing that occurs near the slab-to-column connec-

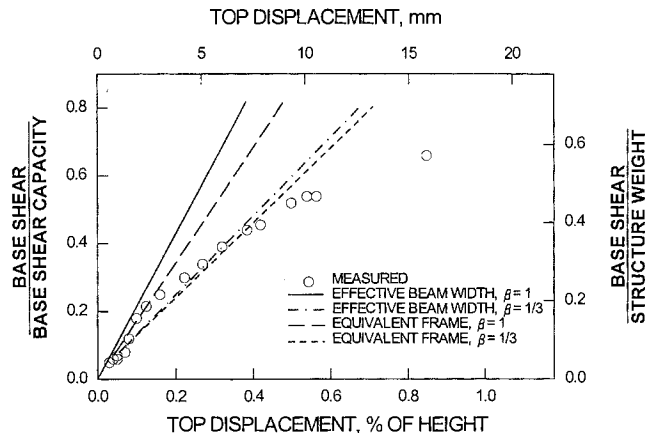


Fig. 11—Comparison between computed and measured lateral load stiffnesses.<sup>20</sup>

tion (as illustrated in Fig. 4(a)), the column and slab-beam members of the equivalent frame are interconnected by torsion members. As described by ACI 318-95,<sup>25</sup> the torsion members may be interpreted to extend with a definite length equal to  $\ell_2$  in the transverse direction.

### Model for lateral load analysis

The ACI Code equivalent frame model was calibrated using data from gravity load tests and analyses,<sup>26-28</sup> and contains elastic properties that are suited to determining design slab moments under gravity loads. In a model having the previously mentioned purpose, relative member stiffnesses are important, and absolute member stiffnesses are not. To properly determine lateral drift and internal forces under lateral load, it is important that absolute stiffnesses be properly represented. Therefore, modifications to the ACI equivalent frame may be necessary if it is to be used for lateral load analysis. Some of the desired modifications are summarized as follows.

One desired modification lies in the definition of the transverse torsion member (Fig. 2). As defined by the ACI Code, the torsion member flexibility is directly proportional to the transverse span length  $\ell_2$ . Because lateral load stiffness is dominated by stiffness of the torsion member, the frame lateral stiffness decreases with increasing transverse span  $\ell_2$ .

To illustrate the effect on lateral stiffness of increasing  $\ell_2$ , the equivalent frame model was used to represent the lateral load stiffness of the frames analyzed previously using the finite element and effective beam width models. As described previously, the frames had the configuration shown in Fig. 7, except the transverse span was varied to obtain a range of span aspect ratios  $\ell_2/\ell_1$ . The results are plotted in Fig. 9 and 10. The equivalent frame model stiffness decreases as the aspect ratio  $\ell_2/\ell_1$ , increases. This finding is contrary to the elastic behavior, as represented by the finite element solution. The finite element model indicates a slight increase in the lateral load stiffness with an increase in  $\ell_2/\ell_1$ , as is expected intuitively.

The effect on stiffness of increasing the transverse span has been noted previously. Vanderbilt and Corley recommended that the length of the torsion member be taken equal to the lesser of the quantities  $\ell_2$  or  $\ell_1$ . The finite element solution of Fig. 9 and 10 suggests that the effect of  $\ell_2$  on lateral load stiffness is negligible throughout the practical range of span aspect ratios  $\ell_2/\ell_1$ . Based on this observation, it is recommended that the length of the transverse torsion member be taken equal to  $\ell_1$ , regardless of the length  $\ell_2$ .

It is apparent in Fig. 9 and 10 that, regardless of the span aspect ratio, the equivalent frame lateral load stiffness is lower than the elastic stiffness, as represented by the finite element solution. This finding is consistent with that of Mehrain and Aal-

Experimental program

To examine issues related to lateral load modeling of reinforced concrete slab-column frames, an experimental program was undertaken. A single-story, reinforced concrete, flat-plate frame with nine panels was built at 4/10 of full scale and tested.<sup>2,3</sup> The configuration of the scaled model is presented in Fig. 7. The slab was tested under gravity and lateral loads. Gravity load tests were designed to observe structural responses at the service load level. Lateral load tests were conducted to monitor service load behavior as well as ultimate capacities. Lateral loads were applied in both the NS and EW directions of the test slab, one direction at a time. Further details can be found in References 2 and 3.

Static design limits of lateral drift ratios are often quoted in a range from 1/700 to 1/300.<sup>13</sup> Corresponding to these criteria, experimental data on lateral stiffness of the test slab at drifts of 1/800, 1/400, and 1/200 will be presented. The tests corresponding to these drift limits are designated (in chronological order) NS800, EW800, NS400, EW400, NS200, and EW200. The letters NS and EW designate loading in the NS and EW directions, respectively. The numeral in the designation is the reciprocal of the drift ratio for that test. Gravity load (including self weight) was 118 lb/ft<sup>2</sup> (5650 Pa). At age of 30 days, an additional load of 55 lb/ft<sup>2</sup> (2630 Pa) had been applied to each panel, one panel at a time, prior to the lateral load tests. Other than this additional loading, construction loads and exposure are believed to have been mild.

Measured lateral secant stiffnesses of test slab are plotted in Fig. 12 and 13. The stiffness reduces steadily as a function of the lateral drift level. Additional details of the behavior are presented elsewhere.<sup>2,3</sup>

Comparison of calculated and measured lateral stiffnesses

Figure 12 and 13 compare measured secant stiffnesses with values obtained from several of the analytical models described previously. The finite element solution is an elastic solution using the mesh shown in Fig. 8. The effective beam width model is assembled with elastic effective beam widths for individual connections defined by Eq. (1) and (2). Effective widths for a given span are taken as the average of effective widths for the contiguous connections. The equivalent frame model is defined in all cases with the torsion member length fixed to the value  $\ell_1$ . The stiffness reduction due to cracking is represented by applying the stiffness reduction of Eq. (3) to the slab-beam of the effective beam width model, and to the torsion member of the equivalent frame model. Also, the equivalent frame model as proposed by Vanderbilt and Corley,<sup>1</sup> having a stiffness reduction factor of 0.33 applied to the slab-beams, is included.

In all cases, the elastic stiffness as represented by the finite element solution exceeds the measured stiffness. Without considering the stiffness reduction factor for cracking, the effective beam width solution also is stiffer than the experiment. As described and discussed previously in relation to Fig. 9 and 10, the elastic effective beam width solution nearly matches the finite element solution for loading in the NS direction, and exceeds the finite element solution for EW loading. The equivalent frame model (without stiffness reduction) reproduces the measured stiffnesses fairly well.

The analytical models in which a stiffness reduction is applied to account for slab cracking meet with varied success (Fig. 12 and 13). The effective beam width model with stiffness reduction defined by Eq. (3) reproduces the measured stiffnesses reasonably well for loading in both directions. The two equivalent frame models, for which a stiffness reduction factor is applied, tend to underestimate the measured stiffnesses.

LATERAL-LOAD STIFFNESS (kip/in.)

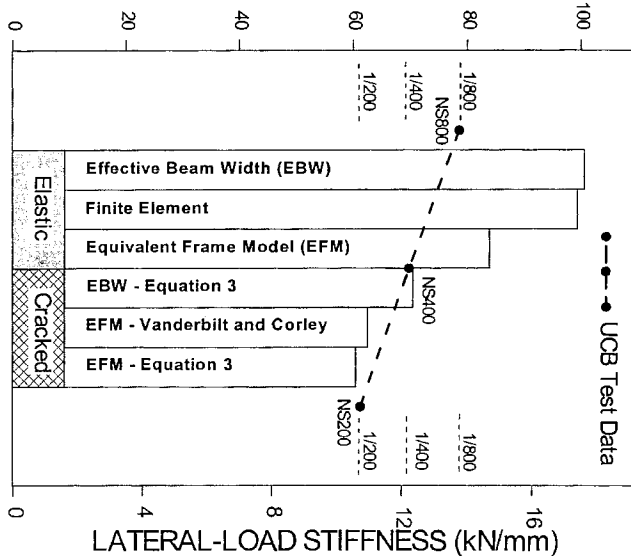


Fig. 12—Lateral stiffnesses of UCB test slab (NS-Dir.).

ami,<sup>9</sup> who proposed a torsion member wider than defined by the ACI Code to match the elastic lateral load solution. This finding is not intended to suggest that the equivalent frame stiffness will be less than actual lateral load stiffness of a reinforced concrete frame. Actual stiffness can be reduced significantly due to effects of slab cracking.

Effects of cracking can be introduced in the equivalent frame model by reducing the torsion member stiffness, by reducing the slab-beam stiffness,<sup>1</sup> or by reducing both stiffnesses in some combination.<sup>29</sup> Under the action of gravity and lateral loads, flexural cracking tends to concentrate near the connection, whereas the slab away from the column tends to remain uncracked. This pattern of cracking suggests it would be most appropriate to apply the stiffness reduction to the torsion member only. Furthermore, in laboratory tests,<sup>2,3</sup> it was observed that connection moments due to gravity loads decreased as damage accumulated due to gravity and lateral loads. The redistributed moment accumulated in the positive moment region because of the reduced stiffness of the connections. This behavior can be represented only by decreasing the torsion member stiffness, not by decreasing the slab-beam stiffness.

Based on the preceding arguments, it is proposed to account for stiffness reduction due to slab cracking under service loads by applying a stiffness reduction to the torsion member of the equivalent frame model.

Wherever the stiffness reduction is introduced, it remains to determine its magnitude. Vanderbilt and Corley<sup>1</sup> recommended a stiffness reduction factor of 1/3 (to be applied to the slab-beam). Equation (3) and (4) recommend a stiffness reduction factor that is suitable for the effective beam width model, the factor being bounded on the lower end by the same value of 1/3. If this factor is applied to the torsion member of the equivalent frame only (rather than the torsion member and the slab-beam), the net stiffness reduction for the equivalent frame will be less than it was for the effective beam width model, as only a portion of the elements representing the slab stiffness is effected. As noted previously and shown in Fig. 9 and 10, however, the equivalent frame model without stiffness reduction tends to be more flexible than the elastic solution. Thus, with the stiffness reduction applied to the torsion member only, it is likely that the resulting stiffness will be reasonable. The result is evaluated by comparison with experimental data in the following section.

EXPERIMENTAL EVALUATION OF LATERAL LOAD

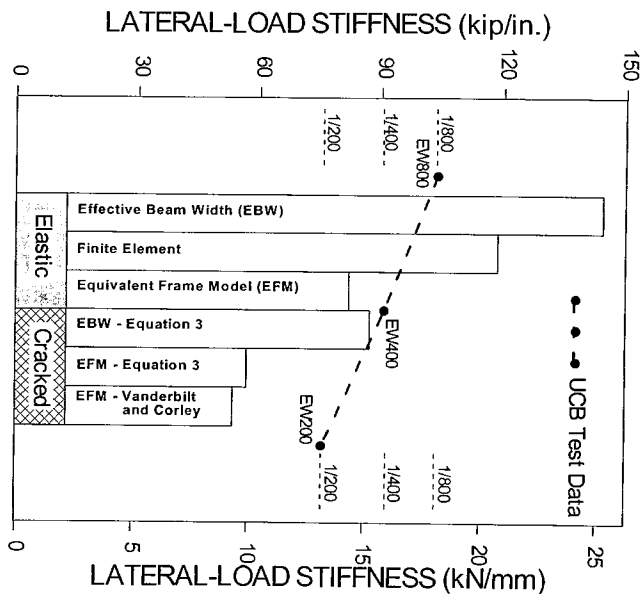


Fig. 13—Lateral stiffnesses of UCB test slab (EW-Dir.).

### SUMMARY AND CONCLUSIONS

The effective beam width and equivalent frame models for lateral load analysis of slab-column frames are described. Results of the models are evaluated by comparison with finite element solutions and with experimental data. Based on the evaluation, the following conclusions are reached.

Elastic analytical studies indicate that within the practical range of slab configurations, the lateral load stiffness is effectively independent of the slab transverse span length  $\ell_2$  and the column transverse dimension  $c_2$ . Recognizing this independence, it is possible to express effective beam widths for the effective beam width model as a simple linear function of the slab longitudinal span  $\ell_1$  and the column longitudinal dimension  $c_1$ . Similarly, to model this behavior using the equivalent frame model, the length of the transverse torsion member should be taken equal to  $\ell_1$ , regardless of the transverse span length  $\ell_2$ .

Both the effective beam width and the equivalent frame models can be suitable models for lateral load behavior of slab-column frames in the elastic range. Both have shortcomings, however. The effective beam width model will produce calculated stiffnesses exceeding the true elastic stiffness for irregular frames, including frames having variations in spans and in column cross sections. The equivalent frame model tends to produce calculated stiffnesses less than the true elastic stiffness.

That neither the effective beam width model nor the equivalent frame model match the true elastic response is of little consequence in design, because reinforced concrete slab-column construction generally has stiffness less than the true elastic stiffness. Stiffnesses measured in the laboratory reduce steadily as lateral drifts increase. An approximate lower bound to the measured stiffness can be obtained using the effective beam width model having beam stiffness reduced to 1/3 of the elastic value. Similarly, a reasonable lower bound stiffness estimate can be obtained using the equivalent frame method having either the transverse torsion member or the slab-beam stiffness reduced to 1/3 of the elastic value. Measurements of internal forces in an experimental study indicate it was more appropriate to apply the stiffness reduction to the torsion member than to the slab-beam.

### ACKNOWLEDGMENTS

Funding for the research was provided mainly by the Reinforced Concrete Research Institute (Task 51) and the University of California at Berkeley. Additional funding was obtained through generous donations from the following firms: Robert Rosenwasser Associates, New York; Rose Associates, New York; S & A Concrete Co., Inc., New York; Timko Contracting Corp., New York; and Harry Macklowe Real Estate Co., Inc., New York. Opinions, findings, conclusions, and recommendations in this paper are

those of the authors and do not necessarily represent those of the organizations previously mentioned.

### NOTATIONS

$b$	=	effective beam width
$c$	=	dimension of square column
$c_1$	=	dimension of rectangular column parallel to loading direction
$c_2$	=	dimension of rectangular column transverse to $c_1$
$d$	=	diameter of circular column
$E$	=	modulus of elasticity of concrete
$f_c$	=	concrete compressive strength
$f_y$	=	steel yield strength
$H$	=	column height
$h$	=	slab thickness
$I$	=	flexural moment of inertia per unit width
$LL$	=	service live load in units of lb/ft <sup>2</sup>
$\ell$	=	length of span of square panel
$\ell_1$	=	length of span parallel to loading direction
$\ell_2$	=	length of span transverse to $\ell_1$
$M$	=	transfer moment acting at column center
$r$	=	distance measured from center of circular column
$x$	=	horizontal coordinate
$y$	=	horizontal coordinate
$z$	=	vertical deflection of slab, positive downward
$\beta$	=	factor of connection stiffness reduction
$\theta$	=	connection rotation
$\nu$	=	Poisson's ratio

### REFERENCES

- Vanderbilt, M. D., and Corley, W. G., "Frame Analysis of Concrete Building," *Concrete International*, V. 5, No. 12, Dec. 1983, pp. 33-43.
- Hwang, S. J., and Moehle, J. P., "An Experimental Study of Flat-Plate Structures under Vertical and Lateral Loads," *Report No. UCB/EERC-93/03*, Earthquake Engineering Research Center, University of California, Berkeley, Feb. 1993, 278 pp.
- Hwang, S. J., and Moehle, J. P., "Vertical and Lateral Load Tests of a Nine-Panel Flat-Plate Frame," *ACI Structural Journal*, V. 97, No. 1, Jan.-Feb. 2000, pp. 193-203.
- Aalami, B., "Moment-Rotation Relation between Column and Slab," *ACI JOURNAL, Proceedings* V. 69, No. 5, May 1972, pp. 263-269. Also, discussion by J. Carpenter, V. 69, No. 11, Nov. 1972, pp. 706-707.
- Allen, F. H., and Darvall, P., "Lateral Load Equivalent Frame," *ACI JOURNAL, Proceedings* V. 74, No. 7, July 1977, pp. 294-299.
- Brotchie, J. F., and Russell, J. J., "Flat Plate Structures," *ACI JOURNAL, Proceedings* V. 61, No. 8, Aug. 1964, pp. 959-996. Also, Part 2 containing development of A, B Factors, American Concrete Institute, 16 pp.
- Carpenter, J. E., "Flexural Characteristics of Flat Plate Floors in Buildings Subjected to Lateral Loads," PhD thesis, Purdue University, West Lafayette, Ind., June 1965, 203 pp.
- Khan, F. R., and Sbarounis, J. A., "Interaction of Shear Walls and Frames," *Proceedings, ASCE*, V. 90, ST3, Part 1, June 1964, pp. 285-335. Also, discussion by Y. Yamamoto, Feb. 1965, p. 317, and closure, Apr. 1966, p. 389.
- Mehrain, M., and Aalami, B., "Rotational Stiffness of Concrete Slabs," *ACI JOURNAL, Proceedings* V. 71, No. 9, Sept. 1974, pp. 429-435.
- Pecknold, D. A., "Slab Effective Width for Equivalent Frame Analysis," *ACI JOURNAL, Proceedings* V. 72, No. 4, Apr. 1975, pp. 135-137. Also, discussion by F. H. Allen and P. Darvall, R. Glover, and author, *Proceedings* V. 72, No. 10, Oct. 1975, pp. 583-586.
- Tsuboi, Y., and Kawaguchi, M., "On Earthquake Resistant Design of Flat Slabs and Concrete Shell Structures," *Proceedings, Second World Conference on Earthquake Engineering*, Science Council of Japan, Tokyo, 1960, V. 3, pp. 1693-1708.
- Wong, Y. C., and Coull, A., "Effective Slab Stiffness in Flat Plate Structures," *Proceedings, Institution of Civil Engineers*, London, Part 2, V. 69, Sept. 1980, pp. 721-735.
- Vanderbilt, D., "Equivalent Frame Analysis of Unbraced Reinforced Concrete Buildings for Static Lateral Loads—EFRAME," *Structural Research Report No. 36*, Colorado State University, July 1981.
- Darvall, P., and Allen, F. H., "Lateral Load Effective Width of Flat Plates with Drop Panels," *ACI JOURNAL, Proceedings* V. 81, No. 6, Nov.-Dec. 1984, pp. 613-617.
- Westergaard, H. M., and Slater, W. A., "Moments and Stresses in Slabs," *ACI JOURNAL, Proceedings* V. 17, 1921, pp. 415-538.
- Banchik, C. A., "Effective Beam Width Coefficients for Equivalent Frame Analysis of Flat-Plate Structures," ME thesis, University of California at Berkeley, Calif., May 1987, 56 pp.
- Allen, F. H., "Lateral Load Characteristics of Flat Plate Structures," MSc thesis, Monash University, Australia, June 1976, 167 pp.

18. Botoz, J. L., and Tahar, M. B., "Evaluation of a New Quadrilateral Thin Plate Bending Element," *International Journal for Numerical Methods in Engineering*, V. 18, 1982, pp. 1655-1677.
19. Wilson, E. L., "The SAP-80 Series of Structural Analysis Programs," Version 84.00, SAP, Inc., El Cerrito, Calif., Jan. 1983.
20. Moehle, J. P., and Diebold, J. W., "Lateral Load Response of Flat-Plate Frame," *Journal of Structural Engineering*, ASCE, V. 111, No. 10, Oct. 1985, pp. 2149-2164.
21. Morrison, D. G.; Hirasawa, I.; and Sozen, M. A., "Lateral-Load Tests of R/C Slab-Column Connections," *Journal of Structural Engineering*, ASCE, V. 109, No. 11, Nov. 1983, pp. 2698-2714.
22. Mulcahy, J. F., and Rotter, J. M., "Moment Rotation Characteristics of Flat Plate and Column Systems," *ACI JOURNAL, Proceedings* V. 80, No. 2, Mar.-Apr. 1983, pp. 85-92.
23. Pan, A., and Moehle, J. P., "Reinforced Concrete Flat Plates under Lateral Load: An Experimental Study Including Biaxial Effects," *Report* No. UCB/EERC-88/16, Earthquake Engineering Research Center, University of California, Berkeley, Oct. 1988.
24. ACI Committee 318, "Building Code Requirements for Reinforced Concrete (ACI 318-83) and Commentary (318R-83)," American Concrete Institute, Farmington Hills, Mich., 1983, 266 pp.
25. ACI Committee 318, "Building Code Requirements for Structural Concrete (ACI 318-95) and Commentary (318R-95)," American Concrete Institute, Farmington Hills, Mich., 1995, 369 pp.
26. Corley, W. G., "Equivalent Frame Analysis for Reinforced Concrete Slabs," PhD thesis, University of Illinois at Urbana-Champaign, 1961, 166 pp. Also issued as Civil Engineering Studies, *Structural Research Series* No. 218, Department of Civil Engineering, University of Illinois, Urbana, Ill.
27. Corley, W. G., and Jirsa, J. O., "Equivalent Frame Analysis for Slab Design," *ACI JOURNAL, Proceedings* V. 67, No. 11, Nov. 1970, pp. 875-884. Also, discussion by Eberhardt and Hoffman, Huang, Jofriet and Handa, and author's closure, May 1971, pp. 397-401.

28. RCRC, "Reinforced Concrete Floor Slabs—Research and Design," *Bulletin No. 20*, Reinforced Concrete Research Council, American Society of Civil Engineers, New York, 1978.

29. Cano, M. T., and Klingner, R. E., "Comparison of Analysis Procedures for Two-Way Slabs," *ACI Structural Journal*, V. 85, No. 6, Nov.-Dec. 1988, pp. 597-608.

## APPENDIX

### Effective Beam Width by Infinite Plate Theory

Westergaard [15] presented the infinite plate theory for flat plates with an infinite number of square bays and circular columns in 1921. Considering an interior flat-plate panel subjected to a transfer moment,  $M$ , acting in the center of a circular column (Figure A1), the displacement fields with zero Poisson's ratio for that moment  $M$  resisted by a column-supported slab are defined as [2]

$$z = \frac{M}{4\pi E \hat{I}} x \left[ \ln\left(\frac{\ell}{2r}\right) - \frac{d^2}{8r^2} + \frac{1}{2}\left(\frac{d}{\ell}\right)^2 \right] \quad (A1)$$

where  $r = \sqrt{x^2 + y^2}$ , and  $\hat{I}$  = the moment of inertia of the slab per unit width.

The connection rotation  $\theta$  due to the transfer moment  $M$  is

$$\theta = \left[ \frac{\partial z}{\partial x} \right]_{@ x=0 \& y=\frac{d}{2}} = \frac{M}{4\pi E \hat{I}} \left[ \ln\left(\frac{\ell}{d}\right) + \frac{1}{2}\left(\frac{d}{\ell}\right)^2 - \frac{1}{2} \right] \quad (A2)$$

The rotational stiffness of the slab estimated by the infinite plate solution is thus

$$\left[ \frac{M}{\theta} \right]_{slab} = \frac{4\pi E \hat{I}}{\left[ \ln\left(\frac{\ell}{d}\right) + \frac{1}{2}\left(\frac{d}{\ell}\right)^2 - \frac{1}{2} \right]} \quad (A3)$$

The derivation applies to a circular column of diameter  $d$ . Replacing the circular column with a square column having width  $c = \frac{d}{\sqrt{2}}$  (so that corners of the square column coincide with the perimeter of the circular column), the rotational stiffness of the square column can be approximated as

$$\left[ \frac{M}{\theta} \right]_{slab} = \frac{4\pi EI}{\left[ \ln\left(\frac{\ell}{c\sqrt{2}}\right) + \left(\frac{c}{\ell}\right)^2 - \frac{1}{2} \right]} \quad (A4)$$

A simply supported equivalent beam, with the transfer moment applied at the rigid joint (size of  $c$ ) in the midspan, has the rotational stiffness as

$$\left[ \frac{M}{\theta} \right]_{beam} = \frac{12EIb}{\ell_1} \frac{1}{\left(1 - \frac{c}{\ell_1}\right)^3} \quad (A5)$$

where  $b$  = the effective beam width, and  $\ell_1$  = the longitudinal span length.

By equating Equations A4 and A5, the effective beam width of the slab-column connection is stated as

$$\frac{b}{\ell_1} = \frac{\pi}{3 \left[ \ln\left(\frac{\ell_1}{c\sqrt{2}}\right) + \left(\frac{c}{\ell_1}\right)^2 - \frac{1}{2} \right]} \left(1 - \frac{c}{\ell_1}\right)^3 \quad (A6)$$

Figure A2 presents results of Equation A6. The results are checked for several column sizes using the finite element method. Results from the various solution compare closely (Figure A2).

Recognizing the near linearity of the curves in Figure A2, Equation A6 can be simplified. A best linear fit to replace the curve of Equation A6 for square columns within the range of values of  $c/\ell_1$  from 0.05 to 0.15 is

$$\frac{b}{\ell_1} = 1.84 \left(\frac{c}{\ell_1}\right) + 0.33 \quad (A7)$$

Without sacrificing much accuracy, Equation A7 can be further simplified to

$$\frac{b}{\ell_1} = 2 \left(\frac{c}{\ell_1}\right) + \frac{1}{3} \quad (A8)$$

## Effective Beam Width by Finite Element Method

Effective widths for edge, corner, and interior connections, have been reported by Banchik [16]. Results of that study are summarized here.

A set of different aspect ratios  $l_1 / l_2$  and  $c_1 / l_2$  were selected by Banchik [16] to encompass ratios commonly used in practice. Aspect ratios ranged from

$$l_1 / l_2 = 0.67, 1.00, 1.50$$

$$c_1 / l_2 = 0.06, 0.09, 0.12$$

Square columns were used in all cases. For all edge and corner connections, two series of analyses were performed. In one series, the plate edge was flush with the outside face of the column. In a second series, overhangs were added in order to evaluate their influence on the effective beam widths. Ratios of overhangs evaluated were,

$$\frac{\text{overhang}}{l_1} = \frac{1}{11}, \frac{1}{7}$$

in which the overhang dimension is measured from the outer column face.

Four node QUAD elements in the SAP 80 program [19] were used for analysis. The elements spanned between 100 nodes arranged in a regular mesh. Sensitivity analyses were carried out to ensure reliability of this mesh. A concentrated moment was applied at the center of the joint. Boundaries perpendicular to loading direction were restrained against displacement. Boundaries parallel to loading direction were restrained against rotation about the axes along the boundaries. Element stiffnesses were based on the gross section. Shear deformations were neglected. Poisson's ratio was assumed to be zero. Joints were made effectively rigid, having a stiffness eight orders of magnitude greater than that of a plate element.

For each analysis, the rotation and moment at the center of the column were obtained. The rotational stiffness of the assemblage was thus determined as  $M / \theta$ . Given

rotational stiffness,  $M / \theta$ , the effective beam width coefficients,  $b / \ell_2$ , of rigid joint were obtained. For the interior connections and the edge connections with bending parallel to edge, the coefficient is defined as

$$\frac{b}{\ell_2} = \frac{M}{\theta} \frac{\ell_1}{\ell_2} \frac{1}{Eh^3} \left(1 - \frac{c_1}{\ell_1}\right)^3 \quad (\text{A9})$$

For the corner connections and the edge connections with bending perpendicular to edge, the coefficient is defined as

$$\frac{b}{\ell_2} = 2 \frac{M}{\theta} \frac{\ell_1}{\ell_2} \frac{1}{Eh^3} \left(1 - \frac{c_1}{\ell_1}\right)^3 \quad (\text{A10})$$

Computed effective beam width coefficients ( $b / \ell_2$ ) for the selected connection geometries are displayed in Tables A1 through A4. The values are given for plane frame analysis assuming rigid joint.

Table A1—Interior Connection

$b/l_2$		$l_1/l_2$		
		0.67	1.00	1.50
$c_1/l_2$	0.06	0.331	0.428	0.533
	0.09	0.380	0.488	0.602
	0.12	0.419	0.536	0.653

Table A2—Edge Connection with Bending Perpendicular to Edge

$b/l_2$		flush			overhang (1/11)			overhang (1/7)		
		$l_1/l_2$			$l_1/l_2$			$l_1/l_2$		
		0.67	1.00	1.50	0.67	1.00	1.50	0.67	1.00	1.50
$c_1/l_2$	0.06	0.359	0.451	0.548	0.391	0.527	0.666	0.406	0.531	0.644
	0.09	0.414	0.518	0.622	0.423	0.560	0.694	0.440	0.573	0.691
	0.12	0.454	0.568	0.675	0.484	0.587	0.718	0.466	0.603	0.722

Table A3—Edge Connection with Bending Parallel to Edge

$b/l_2$		flush			overhang (1/11)			overhang (1/7)		
		$l_1/l_2$			$l_1/l_2$			$l_1/l_2$		
		0.67	1.00	1.50	0.67	1.00	1.50	0.67	1.00	1.50
$c_1/l_2$	0.06	0.192	0.237	0.288	0.224	0.302	0.398	0.255	0.344	0.454
	0.09	0.233	0.284	0.339	0.249	0.331	0.432	0.282	0.378	0.495
	0.12	0.269	0.324	0.382	0.270	0.356	0.458	0.302	0.403	0.526

Table A4—Corner Connection

$b/l_2$		flush			overhang (1/11)			overhang (1/7)		
		$l_1/l_2$			$l_1/l_2$			$l_1/l_2$		
		0.67	1.00	1.50	0.67	1.00	1.50	0.67	1.00	1.50
$c_1/l_2$	0.06	0.201	0.250	0.303	0.247	0.340	0.448	0.288	0.395	0.517
	0.09	0.240	0.296	0.352	0.262	0.359	0.469	0.304	0.416	0.542
	0.12	0.270	0.333	0.393	0.271	0.374	0.485	0.314	0.431	0.559

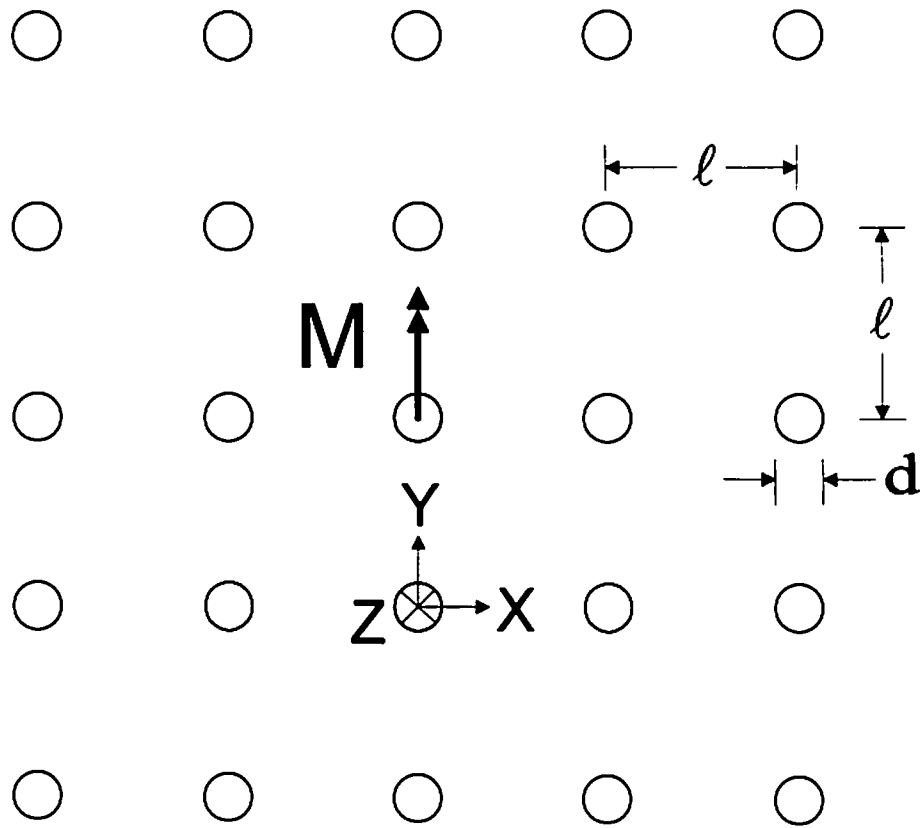


Figure A1 Plan of Infinite Flat Plate with Circular Column

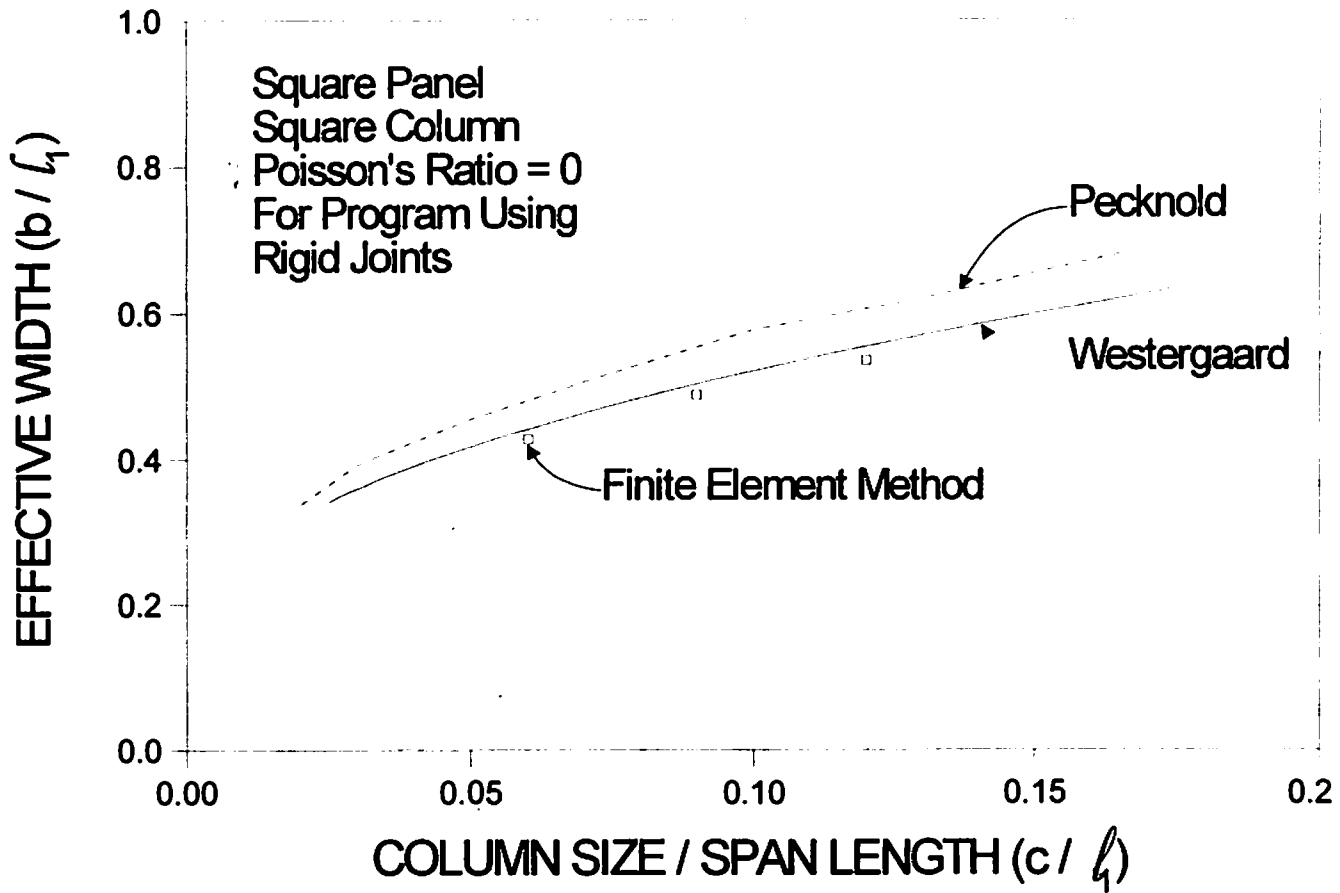


Figure A2 Theoretical Effective Beam Width